

Measuring Tropospheric Propagation in the 21st Century

Adam Hicks

*Institute for Telecommunication
Sciences*

*National Telecommunications
and Information Administration*

Boulder, CO, USA

ahicks@ntia.gov

John Ewan

*Institute for Telecommunication
Sciences*

*National Telecommunications
and Information Administration*

Boulder, CO, USA

jewan@ntia.gov

William Kozma

*Institute for Telecommunication
Sciences*

*National Telecommunications
and Information Administration*

Boulder, CO, USA

wkozma@ntia.gov

Michael Cotton

*Institute for Telecommunication
Sciences*

*National Telecommunications
and Information Administration*

Boulder, CO, USA

mcotton@ntia.gov

Abstract—This article is intended to motivate and describe a new tropospheric scatter modelling and measurement validation effort that is underway at the Institute for Telecommunication Sciences (ITS). Immediately after World War II, there was a flurry of research conducted to investigate the phenomenon of forward scattering through the troposphere, or *troposcatter*, for over-the-horizon radio links. During the early 1950s, ITS researchers carried out an extensive measurement campaign now summarized in the ITS technical report *Cheyenne Mountain Tropospheric Propagation Experiments* [1]. Several propagation models were developed from this effort as well as from similar follow-on measurement campaigns, such as the Irregular Terrain Model (ITM) and IF-77 (ITS-FAA air-to-ground propagation model, circa 1977). These models are based on simplified assumptions, but they are still used in today's spectrum policy decisions. ITS engineers are currently developing a modern measurement system that incorporates the latest RF hardware capabilities and takes advantage of the extensive information now available about our meteorological and geographical environment to improve the accuracy of these models. This paper describes the current and proposed deployments of this modern and upgraded ITS troposcatter measurement system.

Keywords—Historical perspective, IF77, ITM, tropospheric measurement, modeling, propagation modeling, test and validation

I. INTRODUCTION

Midway through the 20th century, over-the-radio-horizon propagation was of keen interest to the world to facilitate long range communication without the cost or logistical concerns of fixed installations. These radio links were made possible through forward scattering effects resulting from electromagnetic waves interacting with inhomogeneities, caused by turbulence, in the troposphere (i.e., the lowest region of the atmosphere, extending from the earth's surface to the lowest boundary of the stratosphere 6 to 20 km in height): a concept colloquially referred to as *troposcatter*.

Troposcatter is sufficiently dependable between 0.3 GHz and 100 GHz that it can be used as a mechanism for long-distance communications [2]. In the 1950s through the 1980s, extensive efforts were focused on deployment of measurement systems to record tropospheric propagation characteristics from which empirical models were developed [3]. These efforts established much of our understanding of tropospheric

propagation mechanisms. After the inception of satellite communications during the 1960s, the need to measure and model tropospheric effects faded from interest.

Today, we find ourselves returning to past scientific accomplishments in order to update and validate the results for the modern communications era. We are faced with the problem of a finite spectrum resource, an expanding communication landscape, and a host of critical legacy systems that operate over wide geographical areas. The need to accurately predict complex interactions between modern and legacy systems at over-the-horizon separations is a critical spectrum sharing challenge. Specifically, NTIA's Institute for Telecommunication Sciences (ITS) is engaged in a new initiative [4] to standardize propagation models in the 3.1–4.2 GHz frequency range in support of spectrum-sharing electromagnetic compatibility/interference (EMC/EMI) analyses to inform rulemakings that promote greater utilization and efficiency of the spectrum. We have the opportunity to both validate past models and develop more robust models using more capable modern hardware and measurement techniques. We now have much more information about propagation paths, including 1 m resolution LIDAR databases to describe the terrain and meteorological data directly from weather radars and satellites.

This paper summarizes pertinent troposcatter concepts, describes significant past efforts to measure tropospheric propagation, and outlines the challenges of measuring propagation loss in the troposcatter region. Finally, we present an ITS-developed measurement system design, and plans to carry out troposcatter measurement campaigns over the next four years (2023–2027).

II. A (BRIEF) INTRODUCTION TO TROPOSCATTER

A basic radio communication path consists of a transmitter and receiver at some distance from each other linked by electromagnetic signals at a selected frequency. It is the pursuit of many radio-frequency (RF) engineers to effectively predict (using a developed model) the characteristics of radio propagation between the two terminals and estimate what effects these characteristics will have on propagation over the relevant area before the (often-arduous) process of installing the terminals. A common metric used by these engineers is the link budget between terminals, which depends on the basic transmission loss of a path and is a desirable value to know in advance. This value helps gauge where other networks can reside, what data transfer rates can be supported, and what steps

The work described in this paper is part of a five-year propagation model study and development program funded by the U.S. Department of Defense Chief Information Officer on a cost-reimbursable basis.

might need to be taken to reduce unplanned electrical interactions. The better our predictive models, the more efficient and reliable our networks become. Both propagation and atmospheric models must be considered for accurate prediction.

Fig 1. reproduces the left side of [5, Fig. 8], which illustrates that as the distance between the terminals increases, the slope of the predicted basic transmission loss (BTL) changes. It is beneficial to subdivide the model into regions based on the mode of propagation that attributes the lowest attenuation to the signal along the path. The line of sight (LOS), diffraction, and troposcatter regions are determined by the location of the terminals and associated path geometries. Each region can be roughly associated with a change in slope in Fig. 1. The troposcatter region is modeled by interactions within the common scattering volume shared by the two antennas. Dalke [6] provides a concise description of this in [6, Eq 21], rewritten here as Eqs (1)-(3), that models troposcatter gain within the common volume, visualized in the shaded blue region of Fig. 2.

Every element of (1)-(3) is associated with the physical parameters present in an over-the-horizon propagation link, albeit with carefully chosen assumptions. Two expressions within the integral are of particular interest for our discussion, as they highlight the reliance on the physical geometry of the link and the influence of atmospheric effects. The G_i expressions describe the antenna gains of the terminals, notably dependent on the effective height of the terminal antennas, h_{ei} , and elevation angles of the rays above the horizon, ψ_i . The term S is an expression of the spectral density function, where S_0 and γ are reliant on the surface refractivity.

$$V^2 = \frac{4l^2}{\pi^2 k} \iiint G_1 G_2 \frac{1}{r_1^2 r_2^2} S dx \quad (1)$$

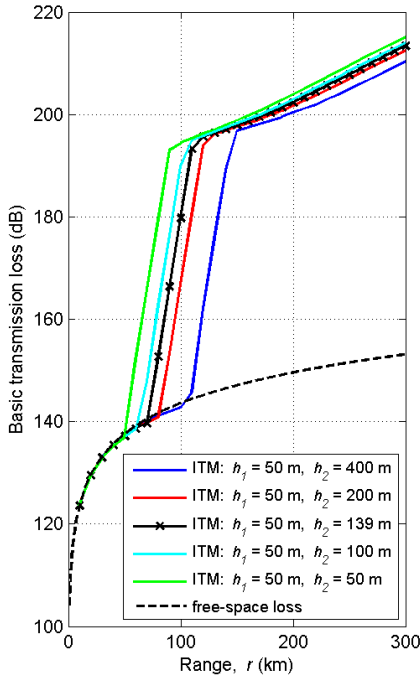


Fig. 1. Irregular Terrain Model (ITM) predictions of basic transmission loss at a variety of terminal heights [1, Fig.8].

$$G_i = \sin^2(kh_{ei} \sin \psi_i), \quad i=1,2 \quad (2)$$

$$S = \frac{S_0 e^{-2\gamma z}}{(2 \sin \frac{\theta}{2})^5} \quad (3)$$

Refractivity is an important parameter in radio wave propagation, as it influences how the ray bends as it travels through the atmosphere. If a model incorporates ray tracing, it will likely rely on atmospheric models to calculate the refractive index as the rays pass through the layered atmosphere. A common model used in the continental United States is the U.S. Standard Reference Atmosphere, 1976 (USSRA76) [7]. This atmospheric model consists of 25 concentric atmospheric layers around the circle of the Earth. Layer thickness is exponentially stratified, ranging from a layer thickness of 10 meters to 25,000 meters. Each stratified layer has a corresponding refractive index, n_i , which is computed from the model input surface refractivity, N_s , in N-Units.

$$n_i = 1 + 1 \times 10^{-6} N_i \quad (4)$$

$$N_i = N_s e^{(-C_e h_i)} \quad (5)$$

$$C_e = \ln \left(\frac{N_s}{N_s - \Delta N} \right) \quad (6)$$

$$\Delta N = -7.32 e^{(0.005577 N_s)} \quad (7)$$

$$N_s = N_0 * e^{-(0.1057 * h_{sys})} \quad (8)$$

with h_i the height of the i^{th} atmospheric layer, and h_{sys} the average elevation of the link. An average mid-latitude value of N_0 is 301. Other factors influence propagation, such as gaseous absorption, multipath and ducting effects [8] and [9].

III. HISTORIC TROPOSCATTER MEASUREMENTS

Table 1 provides a short list of some important troposcatter measurement campaigns and their test frequencies. These

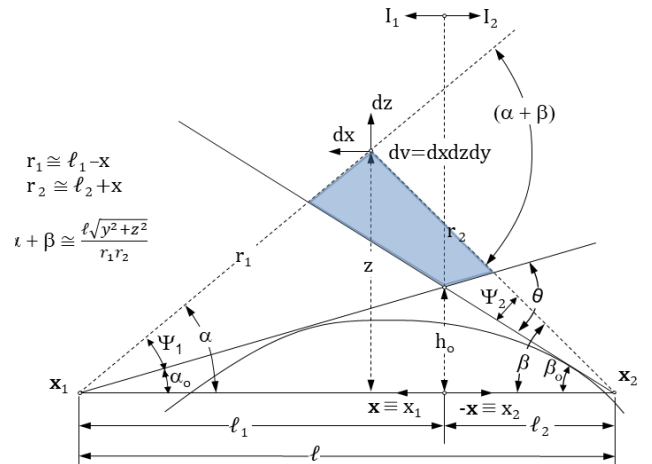


Fig. 2. Geometry for scattering common volume integral.

experiments were designed to capture a variety of conditions related to tropospheric communication ranging from angular scattering and multipath using pulsed signals at 3670 MHz at 303 km to long range, high powered transmissions at very-high frequency (VHF) and ultra-high frequency (UHF) using large parabolic antennas on paths between 322 and 644 km [10].

One significant effort that demonstrates the scope and complexity of troposcatter measurements occurred at Cheyenne Mountain Field Station in Colorado Springs, CO [1]. In 1950, the National Bureau of Standards (NBS) set up over the horizon links to better understand the tropospheric propagation characteristics along several radio paths at 50 MHz to 30,000 MHz. The study selected two permanent transmission sites at Cheyenne Mountain, one about halfway up the mountain (2377 m) and the other at the summit (2682 m).

The campaign also established intermittent locations at Camp Carson (at the base of Cheyenne Mt. at 1890 m) and at the summit of Pikes Peak (at 4298 m). The transmission sites were selected due to the local geography at the eastern slope of the Front Range of the Rocky Mountains, which best simulated air-to-ground paths that were of particular interest to the group. The sites operated continuous wave (CW) transmitters at frequencies around 100, 200, and 1000 MHz, with multiple antenna heights at each frequency. Limited terrain profiles sourced from surveys were available to inform calculations concerning path geometries.

The receiving locations were selected along a radial of approximately 105° east of true north, with locations spaced at distances to capture line of sight, at radio horizon, and just beyond radio horizon records. These permanent locations were at Kendrick, CO; Karval, CO; Haswell, CO; and Garden City, KS, at respective distances of 79.34 km, 112.98 km, 155.46 km and 364.5 km from the transmit sites, pictured in Fig 3. Two additional facilities were considered “semi-permanent”, in that they had different installed infrastructure (only at select frequencies) and were not present for the entire measurement duration. They were located in Anthony, KS, and Fayetteville, AR with distances from the transmit sites of 633.28 km and 994.1 km, respectively, each well beyond the radio horizon.

To reach these distances, the transmitters used a combination of 3 kW VHF commercial transmitters for lower frequency operations and a 4 kW UHF transmitter with a klystron output tube which was custom built for the National Bureau of Standards. At the time, this transmitter was “unique in having the highest continuous power output of any 1,000 MHz transmitter in the country”. It consisted of a crystal driver unit, klystron power amplifier, the direct current-power supplies, and the antenna system. The antenna system was a horn-type radiator designed to minimize ground and local reflections and offer sufficient directive gain at 1,000 MHz. Due to the high

costs associated with development, there was only one system available for the study. It transmitted at a frequency of 1,046.4748 MHz and was located at the Cheyenne Mountain summit facility, along with two commercial transmitters that were designed to operate at 100 MHz and 192.8 MHz (eventually changed to 230 MHz). The Cheyenne Mountain base (halfway up the mountain) hosted two commercial transmitters with frequencies at 92 MHz, and 210.4 MHz (eventually changed to 236 MHz). All commercial transmitters used corner-reflector-type antenna systems to provide directivity into the tropospheric channel. The intermittent sites at Camp Carson and Pikes Peak utilized transmitters at 100 MHz with rhombic and Yagi type antennas, respectively.

It was critical that the transmitters maintain precise frequency discipline throughout operation, as the receiving systems did not have wide bandwidths by today’s standards. They accomplished this by using direct crystal control in combination with suitable multipliers with a second frequency standard. To ensure stable output power, the VHF transmitters were calibrated against water loads and monitored.

Receiver sensitivity was a key parameter for successful system operation. The final design resulted in a receiver with a bandwidth of up to 500 Hz and an overall system noise figure (NF) of between 6 and 11 dB. The exact NF values depended on the center frequency of the receiver. Calibration was performed by occasional checks against a “suitable reference signal generator”. Dipole antennas were used at receive sites in Kendrick, Karval, Haswell, and Garden City. In Anthony, a variety of rhombic antennas were used at VHF, with directive gains ranging from 12 to 18.6 dBi. A Yagi-type antenna was used in the mobile experiments, and a parabolic reflector dish with gain of 25.65 dBi was used at 1,046 MHz. The Fayetteville facility only received frequencies around 100 MHz with rhombic antennas, and it had another parabolic reflector dish set up for the UHF reception.

An interesting addition to the system was the method by which continuous records were kept without supervision. The system designers were limited to analog devices and needed creative solutions to record their results remotely. They used recording milliammeters driven from specially designed receiver output circuits, in conjunction with time-totalizing equipment to track rapid signal variations. The time-totalizers were paired with relay operated cameras, set to snap a photo of

TABLE I. NOTABLE TROPOSCATTER MEASUREMENT CAMPAIGNS FROM THE 1950S

Notable Troposcatter Measurement Campaigns from the 1950s	
Agency	Center Frequency
National Bureau of Standards	100, 200 and 1047 MHz
Bell Telephone Laboratories	3675-3700 MHz
Lincon Laboratories at M.I.T.	3670 MHz
Naval Electronics Laboratory	9375 MHz

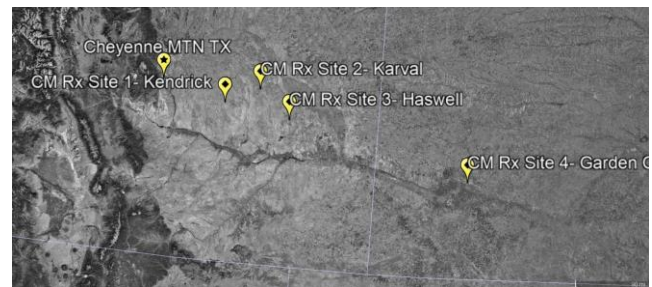


Fig. 3. Cheyenne Mountain transmission paths: (from left) Cheyenne Mountain Transmit Location, Site 1: Kendrick, CO, Site 2: Karval, CO, Site 3: Haswell, CO, Site 4: Garden City, KS. Not pictured: Anthony, KS, and Fayetteville, AR.

counters that tracked time spent at various voltage thresholds. The results were data in both graphical and photo formats.

A critical component to this work was the implementation of meteorological recording devices along the transmission paths. At each site along the path, records of surface temperature, humidity, and pressure were obtained by conventional recording devices. A 152.4 m tower was installed at the Haswell site to capture more detailed meteorological data. This tower was outfitted with equipment to measure the refractive index, wind direction and velocity, scale of turbulence, temperature, barometric pressure, relative humidity, and solar radiation. To ensure an accurate refractive index, they adopted a precision microwave refractometer to aid in this effort. The instruments were installed at heights of 1.5, 4.6, 15.2, 45.7, 91.4 and 152.4 m. These fixed installations were supported by mobile efforts using radiosondes and aircraft to capture similar information along the transmission path.

As the distance between transmit and receive locations increases, the atmosphere has a greater effect on radio wave propagation; therefore, understanding the properties of the troposphere is critical. The study took two approaches in their analysis of wave propagation. The first was to correlate the simultaneous meteorological data with the radio measurements, as a way of expressing the radio wave propagation as a function of the recorded meteorological characteristics. The other was to study the statistical basis of the radio transmission loss to make meaningful predictions on its behavior through a realized link. Reference [1] goes into greater detail in their analysis and results of the effort, with sections dedicated to within radio horizon, the diffraction region, and far beyond radio horizon.

The efforts to link the preliminary results to theory were successful. One key takeaway from this past study is the use of their measurement results to validate the Booker-Gordon theory of scattering (now commonly referred to as forward scatter or troposcatter) for fields beyond the radio horizon.

IV. TROPOSCATTER MEASUREMENTS SYSTEMS IN THE 21ST CENTURY

The current ITS systems design draws on knowledge gained from past measurement campaigns as well as more recent work [11]. Today, there is a wider variety of robust and stable commercial-off-the-shelf (COTS) equipment. The availability of suitable transmitting and receiving equipment greatly facilitates the integration of measurement systems. However, this is not without complications. Figs. 4 and 5 show block diagrams of the transmitting and receiving portions of a

troposcatter measurement system to be deployed by ITS engineers in various environments over the next four years.

The transmitter consists of a GPS-disciplined frequency-referenced signal generator that feeds into a 200 W amplifier. The amplifier is connected to a parabolic antenna with a beamwidth of 3° and relative gain of 33 dBi. Our first long-term measurement will involve a CW signal at 3.475 GHz. The output power is monitored and reported by a power sensor combined with a power meter. The system includes a weather station recording the local real-time relevant meteorological data including humidity, barometric pressure, and temperature. All components are connected through an ethernet switch and controlled via a Linux based computer. Updates and commands are relayed through an LTE router. The transmit system is designed either to be deployed long term where power and infrastructure are available or to be mounted on a mobile trailer and supplied with a tower and generator, for nomadic measurements.

The receiver system is designed to incorporate multiple parallel systems if required, allowing for additional systems to record simultaneously. The system includes a high gain parabolic antenna, like that used in the transmitter, followed by a RF preselector. This preselector consists of a low noise amplifier with a gain of 29 dB and a NF of 1.3 dB. The preamp is connected behind a 50 MHz wide band pass filter, that has an insertion loss of <1 dB and a NF of 0.7 dB. A noise diode for Y-factor calibration is also housed on a separate channel within the preselector, and it is controlled by a web relay. The output of the 50 MHz filter is connected to a vector signal analyzer (VSA) that converts the measured RF signal to a baseband IQ data stream that is digitized for subsequent post processing and analysis. A GPS-disciplined frequency-reference is used to provide high stability and to ensure high accuracy in the measured frequencies. A separate spectrum analyzer is used to monitor the IF output of the recording signal analyzer for redundancy. A function generator provides a periodic trigger to initiate recording for set lengths of time that are required by the conditions of the measurement and the propagation parameters that are being studied.

Once again, a local weather station recording real time meteorological data is integrated into the system. All system components are connected through an ethernet switch to a Linux based control PC. An onsite server allows for data storage and subsequent post processing. We are relying on available United States Geological Survey (USGS) terrain data with 10 m resolution, supplemented with 1 m resolution LIDAR data

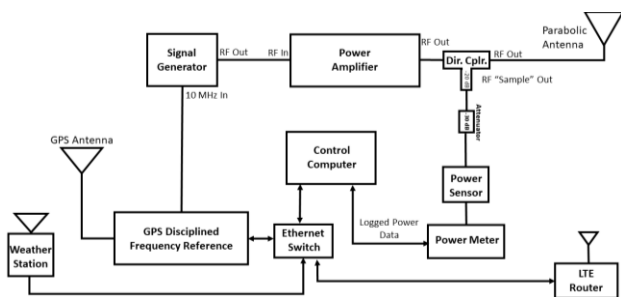


Fig. 4. Figure 4: Block diagram of transmitter system.

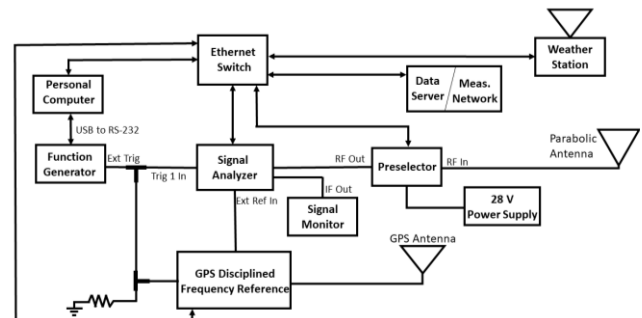


Fig. 5. Block diagram of receiver system.

(where available) to provide terrain profiles between transmitter and receiver locations. Path-wide meteorological data is available through the National Oceanic and Atmospheric Administration (NOAA) using their High-Resolution Rapid Response (HRRR) network. This system provides near-real time meteorological data, on stratified layers in the earth's atmosphere. We can use that information to generate a series of cumulative distribution functions (CDFs) for the refractivity at given crossover heights for specific months of the year. Fig 6 shows the results for the month of December 2021, with a common volume crossover point at 944.8 m above ground level (AGL), located between Longmont, CO, and Eads, CO. The data provided by the NOAA HRRR is far more robust than what was available for the troposcatter investigations of the 1950s.

Initial deployment of the ITS system is currently slated for early summer of 2022. We plan to establish our receive location at the Advanced Communications Test Site at the Table Mountain Radio Quiet Zone in Longmont, CO. Several sites are under consideration for our transmit location. These include Sterling, CO; Julesburg, CO; Limon, CO; and Eads, CO, which fall on radials extending to the northeast and southeast from our receiver. Eads is of interest due to its proximity to Haswell, CO, one of the Cheyenne Mountain campaign sites. Using Eads, CO, as an example, we can expect a median basic transmission loss of 227.3 dB as predicted by ITM. This leaves an estimated SNR of ~18 dB, which is close to our target value of 20 dB. Once deployed, the system will operate continuously for a minimum of 6 months per path. The processed data will be compared to predicted results (Fig. 7) for validation and improvement based on assumptions made during the model development and reflected in the measurement design.

V. SUMMARY

The tropospheric measurements conducted at the Cheyenne Mountain Field Station laid the groundwork for the theoretical and empirical prediction models we use today, and the resulting discussions presented in [12] and [13]. Researchers at the NBS invented new technologies and developed ways to integrate existing hardware into system designs meant to measure over the horizon propagation paths at VHF and UHF. In the 1950s, this was on the frontier of available spectrum and pushed the boundaries of radio science. Over 70 years have passed since these initial measurements were taken. Although the models that

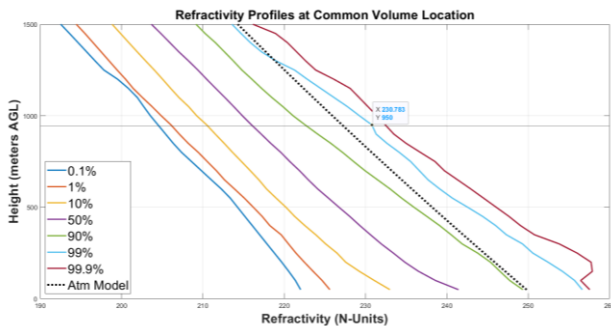


Fig. 7. Refractivity Profiles showing the relationship of common volume height (m-above ground level) on refractivity (N-units) for the month of December 2021 for a range of confidence levels. From left, 0.1%, 1%, 10%, 50%, 90%, (Atmospheric Model: USSRA76), 99%, and 99.9%. Data block highlights X=230.78 at Y=950.

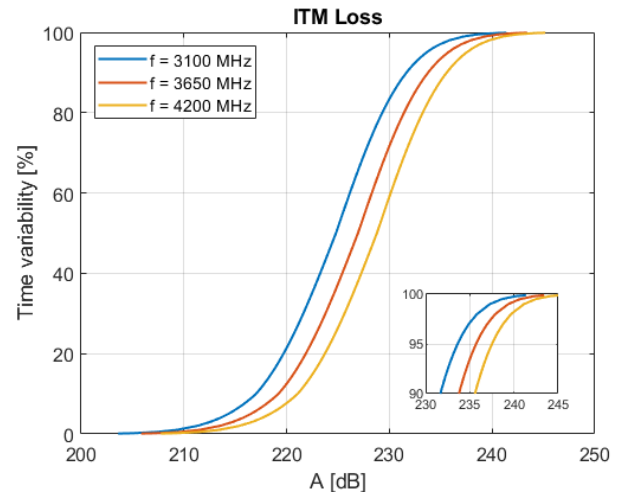


Fig. 6. Time variability (%) of basic transmission loss (dB) as predicted by the Irregular Terrain Model (ITM) at three frequencies. From left: $f = 3100$ MHz, $f = 3650$ MHz, and $f = 4200$ MHz.

were derived from past measurements have been updated, and new methods of prediction have been introduced, it is critical that these models be validated and upgraded against new measured data. Fortunately, radio hardware has improved as the decades have passed, and new data resources are available to characterize the environment and geography of our measured propagation paths. This improvement in hardware fidelity and the availability of high resolution terrain and meteorological data will offer the opportunity to validate and improve these foundational models of the past to bring them forward for the future.

REFERENCES

- [1] A. P. Barsis, J. W. Herbstreit, and K. O. Hornberg, "Cheyenne Mountain Tropospheric Propagation Experiments," U.S. Department of Commerce, National Bureau of Standards, Circular 554, Jan. 1955.
- [2] J. D. Parsons, "Fundamentals of VHF and UHF Propagation," in *Mobile Radio Propagation Channel (2nd edition)*, West Sussex, England: John Wiley & Sons Incorporated, 2000, p. 27.
- [3] W. Hoffman, "The 1953 symposium on tropospheric wave propagation within the horizon at the U. S. Navy Electronics Laboratory," in *Transactions of the IRE Professional Group on Antennas and Propagation*, vol. 1, no. 1, Jul. 1953, pp. 28-30. doi: 10.1109/T-AP.1953.27323
- [4] Interagency Agreement between DoD CIO and NTIA ITS, *DOD-3450-2 ITS Propagation Model Study*, GTC A2106-097-013-011896 (2021)
- [5] M. Cotton, R. Dalke, "Spectrum Occupancy Measurement of the 3550-3650 Megahertz Maritime Radar Band near San Diego, California," U.S. Department of Commerce, National Telecommunications and Information Administration, Technical Report TR-14-500, Jan. 2014. <https://www.its.ntia.gov/publications/2747.aspx>
- [6] R. Dalke, "Tropospheric Scatter: Theory vs Predictive Models," U.S. Department of Commerce, National Telecommunications and Information Administration, Technical Report TR-22-557, Feb. 2022. <https://www.its.ntia.gov/publications/3276.aspx>
- [7] United States Committee on Extension to the Standard Atmosphere, *U.S. Standard Atmosphere, 1976*, U.S. Department of Commerce, National Oceanic and Atmospheric Administration, Oct. 1976. https://www.ngdc.noaa.gov/stp/space-weather/online-publications/miscellaneous/us-standard-atmosphere-1976/us-standard-atmosphere_st76-1562_noaa.pdf

- [8] K. A. Norton and J. B. Wiesner, "The Scatter Propagation Issue," in *Proceedings of the IRE*, vol. 43, no. 10, pp. 1174-1174, Oct. 1955. doi: 10.1109/JRPROC.1955.277931
- [9] P. L. Rice, A. G. Longley, K. A. Norton, and A. P. Barsis, "Transmission loss predictions for tropospheric communication circuits," U.S. Department of Commerce, National Bureau of Standards, Technical Note 101, Vols. 1 and 2, Jan 1967. <https://www.its.ntia.gov/publications/2726.aspx>
- [10] J. Chisholm, "Progress of tropospheric propagation research related to communications beyond the horizon," in *IRE Transactions on Communications Systems*, vol. 4, no. 1, Mar. 1956, pp. 6-16. doi: 10.1109/TCOM.1956.1097265.
- [11] L. C. Colussi, et al. "Multiyear Trans-Horizon Radio Propagation Measurements at 3.5 GHz" in *IEEE Transactions on Antennas and Propagation*, Vol. 66, No. 2, Feb. 2018.
- [12] G. Hufford, "The ITS Irregular Terrain Model, version 1.2.2: The Algorithm," U.S. Department of Commerce, National Telecommunications and Information Administration, unnumbered white paper, Jan 1999. https://its.ntia.gov/media/50676/itm_alg.pdf
- [13] G.D. Gierhart and M.E. Johnson, "The IF-77 Electromagnetic Wave Propagation Model," U.S. Department of Transportation, Federal Aviation Administration, Report DOT/FAA/ES-83-3, Sep. 1983. <https://www.its.ntia.gov/publications/2524.aspx>